The Astrophysical Journal, 984:43 (7pp), 2025 May 1 https://doi.org/10.3847/1538-4357/adc810

Atmospheric Absorption of Dark Matter

Man Ho Chan
Department of Science and Environmental Studies, The Education University of Hong Kong, Hong Kong, People's Republic of China; chanmh@eduhk.hk
Received 2024 December 18; revised 2025 March 25; accepted 2025 March 31; published 2025 April 23

Abstract

Typically, the interaction between dark matter and ordinary matter is assumed to be very small. Nevertheless, in this article, I show that the effective resonant absorption of dark photon dark matter in the atmosphere is definitely possible. This might also be associated with the alleged temperature anomalies observed in our upper stratosphere. By allowing a small amount of additional energy deposition to our upper stratosphere, a narrow dark matter mass range $m_A \sim 0.0001$–0.001 eV and the corresponding range of the mixing parameter ε are constrained for the first time. This proposal might overturn our usual assumption of extremely weak interaction between dark matter and ordinary matter and revive the hope of detecting dark matter directly. Some important implications of this proposal, such as the heating of planets and supermassive dark stars, would also be discussed.

Unified Astronomy Thesaurus concepts: Dark matter (353); Particle astrophysics (96)

1. Introduction

The nature of dark matter is a long-lasting mystery in cosmology. For the most popular candidate weakly interacting massive particles (WIMPs), many direct-detection experiments (e.g., PICO-60, XENON1T, LUX-ZEPLIN, and DEAP-3600) are trying to detect if there is any interaction between WIMP dark matter particles and ordinary matter (D. S. Akerib et al. 2017; E. Aprile et al. 2018, 2023, 2020; C. Amole et al. 2019; J. Aalbers et al. 2023; P. Adhikari et al. 2022). However, the null detection of the dark matter signal makes the problem much more severe. A large parameter space of interaction cross section against dark matter mass has been ruled out, which gives significant tension with the predicted properties of WIMPs from particle physics (E. Aprile et al. 2023; J. Aalbers et al. 2023; G. Arcadi et al. 2024). For indirect detection of WIMP dark matter, no compelling signal has been received either (M. Ackermann et al. 2015; A. Albert et al. 2017; M. Aguilar et al. 2019; M. H. Chan & C. M. Lee 2020; G. Beck & M. Sarkis 2023). Furthermore, for another popular candidate axion dark matter, some cavity experiments using haloscopes (e.g., ADMX, CAPP, and RADES) are also trying to detect if there is any axion-photon conversion signal under a strong magnetic field (O. Kwon et al. 2021; C. M. Adair et al. 2022; ADMX Collaboration 2023; B. Yang et al. 2023; S. Ahyoune et al. 2024). Nevertheless, no such photon signal has been recorded for a large range of axion mass. Although the above results do not rule out the possibility of WIMPs or axions being the major component of cosmological dark matter, they have increased the crisis of incorporating cold dark matter into the standard cosmological model.

Recently, K. Zioutas et al. (2020) reported that the stratospheric temperature shows a strong peak around December–January in each year between 1986 and 2018, which is not correlated with solar activity (K. Zioutas et al. 2020; A. Zhitnitsky & M. Maroudas 2025). Further analysis of the temperature fluctuation in the stratosphere demonstrates a possible correlation with the planetary positions (K. Zioutas et al. 2020). A similar correlation also appears in the total electron content of the Earth's atmosphere (S. Bertolucci et al. 2017). A tiny amount of extra energy deposition $\sim$(0.1–1) W m^{-2} is possible to account for the seasonal variation of the upper stratosphere (i.e., altitude 38.5–47.5 km; K. Zioutas et al. 2020; A. Zhitnitsky & M. Maroudas 2025). One recent study has proposed to explain these puzzles with the model of axion quark nuggets (AQNs) dark matter (A. Zhitnitsky & M. Maroudas 2025). The strong interaction between the AQNs and atmospheric particles can provide the required energy deposition. In fact, the interpretation of the stratospheric temperature anomalies is still uncertain and inconclusive. More follow-up analyses are definitely required to argue how the planetary motion is correlated to the reported anomalies. Nevertheless, this issue has initiated a possibility that dark matter might be able to interact with our atmosphere significantly.

In fact, there is another popular dark matter candidate called dark photon dark matter (DPDM; J. Redondo & M. Postma 2009; A. E. Nelson & J. Scholtz 2011; P. W. Graham et al. 2016; M. Fabbrichesi et al. 2020), which can give modest interaction between dark matter and ordinary matter through kinetic mixing with ordinary photons. In this article, I show that the DPDM could be effectively absorbed by our atmosphere due to resonant absorption, provided that only 0.1–1 W m^{-2} energy deposition is contributed to the upper stratosphere ($<$0.1% of the solar energy flux). It can be shown that a very large portion of DPDM could be absorbed by our atmosphere so that only a very small portion of dark matter particles can strike the ground-based direct-detection experiments and axion haloscopes. I will also discuss some interesting and important implications, which are somewhat consistent with observations and useful in future dark matter searches.

2. The Absorption of DPDM

In particle physics, there is a conjectured dark sector parallel to our own (M. Fabbrichesi et al. 2020). It contains some unknown states that might constitute the cosmological dark matter in our Universe. In view of this, there may exist a kind of photon called dark photons, kinetically mixing with ordinary visible photons. The kinetic mixing between dark photons and ordinary photons provides a possibility to detect dark photons

in experiments. The only parameter involved is the mixing parameter ε.

Generally speaking, dark photons can be massless or massive. A very light, massive dark photon could be a dark matter candidate (i.e., DPDM). DPDM could be produced nonthermally in the early Universe as a condensate, like the axion production mechanism (A. E. Nelson & J. Scholtz 2011; M. Fabbrichesi et al. 2020). They can also be produced in the inflation era (P. W. Graham et al. 2016). When the Hubble constant drops below the DPDM mass, the DPDM field starts to oscillate and behaves like cold dark matter (M. Fabbrichesi et al. 2020). Therefore, in principle, DPDM can form structures and distribute like cold dark matter, which can match the properties observed in large-scale structures and galactic rotation curves. In fact, the DPDM model is currently a popular dark matter model, which has been put on tests in many state-of-the-art experiments and observations (J. Chiles et al. 2022; H. An et al. 2023; F. Bajjali et al. 2023; N. T. Hunt-Smith et al. 2023; H. An et al. 2024; S. Knirck et al. 2024; S. Roy & C. E. M. Wagner 2024). Some positive evidence has been found to favor the existence of dark photons (N. T. Hunt-Smith et al. 2023).

DPDM can interact with ordinary matter through a resonant absorption process (A. Arvanitaki et al. 2018). In particular, DPDM with energy lower than 1 eV can be absorbed by the vibrational and rotational transition in molecules, such as oxygen and water molecules (like the greenhouse effect). The kinetic mixing between DPDM and ordinary photons provides a possibility for the resonant capture of DPDM by an atom or a molecule. For an ordinary photon with frequency ν, the cross section for vibrational and rotational resonant absorption can be written in the following Lorentzian form (E. J. Barton et al. 2017; E. J. Zak 2022):

$$\sigma_r = \frac{Ac^2 g \exp(-E/kT)[1 - \exp(-h\nu/kT)]}{8\pi\nu^2 Q(T)} \times \left[\frac{\Delta\nu}{\pi}\frac{1}{(\nu-\nu_0)^2 + (\Delta\nu)^2}\right], \quad (1)$$

where A is the Einstein coefficient, g is the degeneracy factor, E is the initial energy level, T is the temperature of the molecules, $Q(T)$ is the molecular partition function, $\Delta\nu$ is the frequency width of the absorption, and ν_0 is the resonant frequency. The cross section for DPDM can be obtained in terms of the mixing parameter ε as (M. Fabbrichesi et al. 2020)

$$\sigma_A = \varepsilon^2 \sigma_r. \quad (2)$$

This is assuming there exists a resonant frequency ν_0 in the target molecules, which is very close to the DPDM frequency $\nu = m_A c^2/h$, where m_A is the mass of DPDM. The cross section of DPDM becomes

$$\sigma_A \approx \frac{Ac^2\varepsilon^2}{8\pi^2\nu^2\Delta\nu}\left[1 - \exp\left(-\frac{h\nu}{kT}\right)\right]\left[\frac{g\exp(-E/kT)}{Q(T)}\right]. \quad (3)$$

The Einstein coefficient A is close to the reciprocal of decay lifetime $(\Delta\tau)^{-1}$. Therefore, based on the uncertainty principle, we have $A \sim (\Delta\tau)^{-1} \sim \Delta\nu$. At the stratosphere, the temperature at altitude $\sim$40 km is about 250 K. By taking $g\exp(-E/kT) \approx 1$ and $Q(T) \approx 44$ using water molecules as an example (G. J. Harris et al. 1998), we get

$$\sigma_A = 4.43 \times 10^{-16}\varepsilon^2\left(\frac{m_A}{1\ \text{eV}}\right)^{-2} \times \left[1 - \exp\left(-\frac{46.4 m_A}{1\ \text{eV}}\right)\right]\ \text{m}^2. \quad (4)$$

As dark matter particles are moving inside the Milky Way galaxy as well as the solar system, we expect that there is a dark matter flux passing through our Earth. The dark matter flux is given by (D. A. Neufeld et al. 2018)

$$\Phi = 6 \times 10^{19}\left(\frac{1\ \text{eV}}{m_A}\right)\left(\frac{\rho_{DM}}{0.3\ \text{GeV cm}^{-3}}\right) \times \left(\frac{\langle v\rangle}{200\ \text{km s}^{-1}}\right)\ \text{m}^{-2}\ \text{s}^{-1}, \quad (5)$$

where ρ_{DM} is the DPDM density at the solar position and $\langle v\rangle$ is the average velocity of DPDM. Assuming DPDM follows a Maxwell–Boltzmann distribution, the average velocity of DPDM is

$$\langle v\rangle = \int_0^\infty \frac{4}{\sqrt{\pi}v_p^3} v^3 e^{-v^2/v_p^2} dv = \frac{2v_p}{\sqrt{\pi}}, \quad (6)$$

where v_p is the characteristic velocity. When DPDM is passing through the Earth's atmosphere, we expect that the absorption process of DPDM by the molecules in the atmosphere would occur. If we assume that all DPDM is absorbed by the atmosphere, the maximum energy flux contributed by DPDM would be

$$\dot{E} = \Phi m_A c^2 = 9.6\left(\frac{\rho_{DM}}{0.3\ \text{GeV/cm}^3}\right) \times \left(\frac{\langle v\rangle}{200\ \text{km s}^{-1}}\right)\text{W m}^{-2}. \quad (7)$$

Taking $\rho_{DM} = 0.297\ \text{GeV cm}^{-3}$ constrained from the Gaia data (F. S. Labini et al. 2023) and $v_p = 270\ \text{km s}^{-1}$ (J. F. Acevedo et al. 2024), we get $\dot{E} = 14.6\ \text{W m}^{-2}$. This energy flux is $\sim$10–100 times the required energy deposition to explain the temperature anomaly in our stratosphere.

Although our ultimate goal is not to account for the alleged stratospheric temperature anomalies, we take the required energy deposition 0.1–1 W m^{-2} between the stratospheric layers at latitude 38.5–47.5 km reported in K. Zioutas et al. (2020) and A. Zhitnitsky & M. Maroudas (2025) as our reference to analyze the possible absorption. This tiny additional energy deposition is approximately equivalent to producing a maximum temperature variation of 2.5 K in the upper stratosphere (K. Zioutas et al. 2020). Considering the optical depth of DPDM and assuming the fraction of the absorption molecules containing the resonant frequency $\nu_0 \approx \nu$ is close to one. The optical depth for each DPDM particle traveling from the vertical height $z = \infty$ to an altitude $z = h$ is

$$\tau(h) = \frac{1}{\bar{m}}\int_\infty^h \rho_{\text{atm}}(z)\sigma_A dz, \quad (8)$$

where $\bar{m} = 2.4 \times 10^{-26}$ kg is the average mass of an air molecule in our atmosphere and ρ_{atm} is the mass density of air. By applying the barometric formula, the mass density of air in

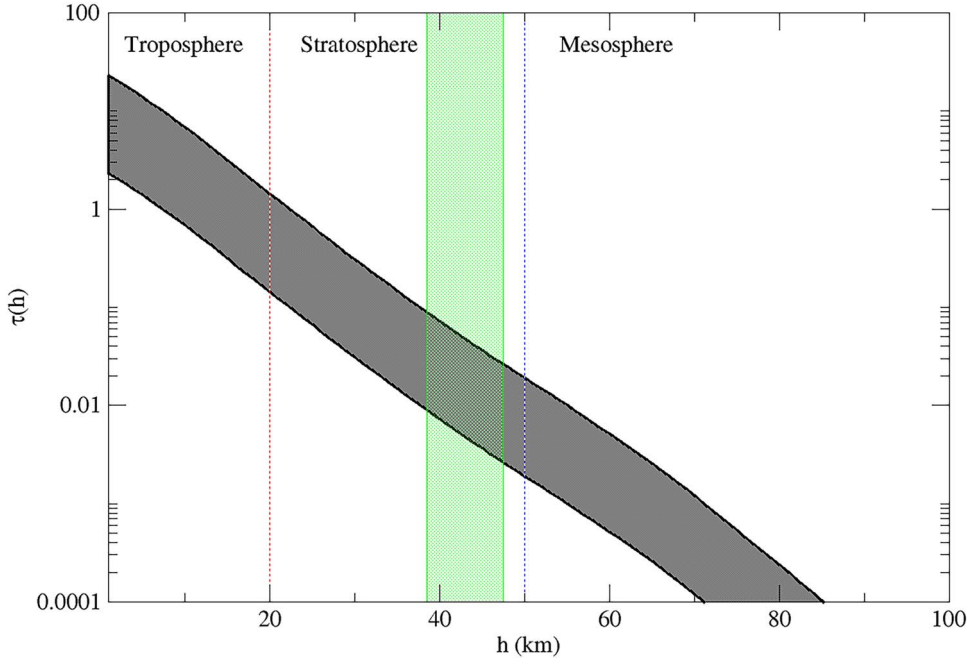

Figure 1. The black shaded band represents the possible range of the optical depth of DPDM $\tau(h)$ from $z = \infty$ to $z = h$ (assumed $\dot{Q} = 0.1 - 1\ \mathrm{W\ m^{-2}}$). The green shaded area indicates the layer (h = 38.5–47.5 km) of the stratospheric temperature anomaly reported in K. Zioutas et al. (2020). Here, we have assumed $\varepsilon^2(m_A/1\ \ \mathrm{eV})^{-2}[1 - \exp(-46.4(m_A/1\ \mathrm{eV}))] = (1.28 - 12.8) \times 10^{-14}$. The dotted lines demarcate different layers of our atmosphere.

troposphere and stratosphere is, respectively, given by

$$\rho_{\mathrm{atm}}(z) = \rho_b\left[\frac{T_b - (z - z_b)L_b}{T_b}\right]^{\frac{g_0 M}{RL_b}-1}, \tag{9}$$

and

$$\rho_{\mathrm{atm}}(z) = \rho_b \exp\left[\frac{g_0 M(z - z_b)}{RT_b}\right], \tag{10}$$

where ρ_b, T_b, and L_b are the standard density, temperature, and lapse rate, respectively, in different successive layers; $g_0 = 9.807\ \mathrm{m\ s^{-2}}$ is the surface gravitational acceleration, $R = 8.314\ \mathrm{N\ m\ mol^{-1}\ K^{-1}}$ is the universal gas constant, and $M = 0.02896\ \mathrm{kg\ mol^{-1}}$ is the molar mass of air. In Figure 1, we plot the variation of $\tau(h)$ for the optical depth constrained by the stratospheric anomalies.

Now we consider the stratospheric absorption between $h = 47.5$ km to $h = 38.5$ km, the atmospheric layer where the energy deposition flux is calculated. By integrating $\int\rho_{\mathrm{atm}}(z)dz$ using the barometric formula, the optical depth from $h = 47.5$ km to $h = 38.5$ km is

$$\begin{aligned}\Delta\tau &= \tau(38.5) - \tau(47.5)\\ &= 5.30 \times 10^{11}\varepsilon^2\left(\frac{m_A}{1\ \mathrm{eV}}\right)^{-2}\\ &\times\left[1 - \exp\left(-\frac{46.4m_A}{1\ \mathrm{eV}}\right)\right].\end{aligned} \tag{11}$$

Since the extra energy deposition in this particular layer is $\dot{Q} \sim 0.1 - 1\ \mathrm{W\ m^{-2}}$ (K. Zioutas et al. 2020; A. Zhitnitsky & M. Maroudas 2025), we get $\Delta\tau = \dot{Q}/\dot{E} = 0.0068 - 0.068$. This can give a narrow possible parameter space of ε and m_A for the DPDM model:

$$\begin{aligned}&\varepsilon^2\left(\frac{m_A}{1\ \ \mathrm{eV}}\right)^{-2}\left[1 - \exp\left(-\frac{46.4m_A}{1\ \ \mathrm{eV}}\right)\right]\\ &= (1.28 - 12.8) \times 10^{-14}.\end{aligned} \tag{12}$$

The allowed ε against m_A (in red shaded band) is plotted in Figure 2. It can be seen that a large region of $\varepsilon - m_A$ parameter space is ruled out by the astrophysical and cosmological bounds, except for the narrow range of dark matter mass $m_A \sim 0.0001$–0.001 eV. In other words, if the stratospheric anomalies are real, DPDM with $m_A \sim 0.0001$–0.001 eV can simultaneously explain the anomalies and satisfy the current astrophysical (e.g., based on JWST observations and solar constraints; N. Vinyoles et al. 2015; S.-P. Li & X.-J. Xu 2023; H. An et al. 2024) and cosmological (e.g., based on cosmic microwave background data; P. Arias et al. 2012; S. J. Witte et al. 2020) bounds. Here, we also include the excluded parameter space of solar dark photons constrained by the XENON1T experiment in E. Aprile et al. (2022) for comparison, because the produced dark photons are relativistic, so that the absorption cross section would be different from that for DPDM. Note that since there is a huge amount of discrete resonant frequencies for molecules, the actual limit on ε should be in the form of many discrete sharp lines. Nevertheless, in Figure 2, we only consider the case of resonant absorption, so the resultant limit of ε in Figure 2 appears continuous. In Figure 3, by considering the rotational excitation energies in oxygen molecules O_2[1], we plot the lower limits of ε for $m_A = 0.0001$–0.004 eV. The positions of the sharp line limits

[1] The data of the rotational excitation photon frequencies for oxygen molecules O_2 are obtained from the Molecular Spectral Databases from National Institute of Standards and Technology.

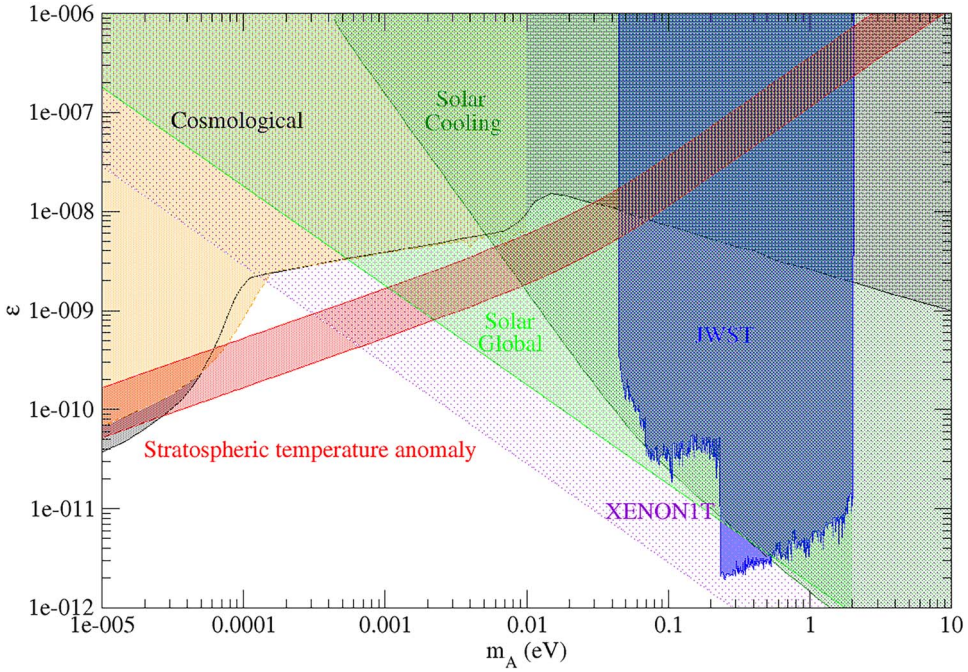

Figure 2. The red shaded band represents the allowed parameter space of ε, assuming $\dot{Q} = (0.1 - 1)$ W m^{-2}. The black and orange shaded regions represent the ruled out parameter space based on the cosmological observations in P. Arias et al. (2012) and S. J. Witte et al. (2020), respectively. The blue, green, and dark green shaded regions represent the ruled out parameter space based on the JWST observations (H. An et al. 2024), solar global analysis (N. Vinyoles et al. 2015), and solar cooling constraints (S.-P. Li & X.-J. Xu 2023), respectively. The violet shaded region represents the ruled out parameter space of solar dark photons based on the XENON1T experiment (E. Aprile et al. 2022).

correspond to the possible resonant energies for rotational excitation due to DPDM absorption. For vibrational absorption, the corresponding m_A for oxygen molecules is greater than 0.24 eV, which is ruled out by other constraints. In general, other air molecules, such as nitrogen and water molecules, could also contribute to DPDM absorption. Here, the lower limit of ε shown in Figure 3 is just a particular example demonstrating the line-shaped limit. All the possible parameter space of $\varepsilon - m_A$ is enclosed by the red shaded region in Figure 2.

On the other hand, in Figure 1, we can see that the total optical depth at $h = 0$ is $\tau(0) \sim 2.2$–22, which means that almost all DPDM particles would be absorbed in our atmosphere. Therefore, the dark matter flux that can continue to pass through the Earth's crust and also the resonant cavity apparatus used in the detection experiments would be largely suppressed. This might explain why we cannot detect any signal of dark matter using the direct-detection experiments and cavity experiments. The existing experimental bounds on ε (A. Caputo et al. 2021) would need to be significantly revised because the actual number of dark matter particles passing through the experimental apparatus is much overestimated. Therefore, in this context, the bounds on ε using direct-detection experiments (E. Aprile et al. 2023) and cavity experiments (ADMX Collaboration 2020) are no longer viable, so we do not include the corresponding bounds in Figure 2. Nevertheless, the astrophysical and cosmological bounds are still applicable for constraining ε as the corresponding data are not affected by our atmosphere.

3. Other Important Implications

There are some interesting implications if DPDM can be effectively absorbed by ordinary matter. In the interstellar medium, the number density is too low ($n \sim 1$–$10\,\mathrm{cm}^{-3}$) so that the absorption of DPDM is not effective. Nevertheless, in planets, stars, or dense clouds, the heating of dark matter might be significant. Also, as a larger DPDM flux can be found at a higher altitude (not yet absorbed), there is a new possible way for direct dark matter detection.

3.1. Heating of Planets

In planets and stars, the density is high enough for DPDM to be absorbed. A large amount of DPDM would first heat up the atmosphere and then the planetary or stellar body. However, in stars, the energy generated by nuclear fusion is much larger than the dark matter heating. Therefore, the stellar heating due to DPDM is negligible. Nevertheless, in planets, the power absorbed from the host star might be comparable to the dark matter heating rate. Consider our solar system. The solar luminosity flux goes like $1/r^2$ while the dark matter heating flux is almost constant (neglecting the effect of planetary motion). In Figure 4, we plot the energy flux as a function of the distance from the Sun. One can see that dark matter heating becomes important in Jovian planets. Coincidentally, many studies have indicated that there is internal heating found in Jupiter (with the rate $\dot{Q} = 7.485 \pm 0.163$ W m^{-2}; L. Li et al. 2018), Saturn (A. P. Ingersoll 2020), Neptune (S. Markham & D. Stevenson 2021), and Pluto (A. Witze 2015). Also, the high temperature at the center of Uranus might indicate a nonadiabatic process (B. A. Neuenschwander et al. 2024). Internal heating can also be found recently in exoplanets (L. Welbanks et al. 2024). Although there are several possible known internal heating sources, such as tidal heating and radioactive decay, heating the planets by DPDM may also be a possible origin. Moreover, dark matter heating might also contribute to the energy input in the planetary atmosphere to cause temperature inversion. Such a temperature inversion can

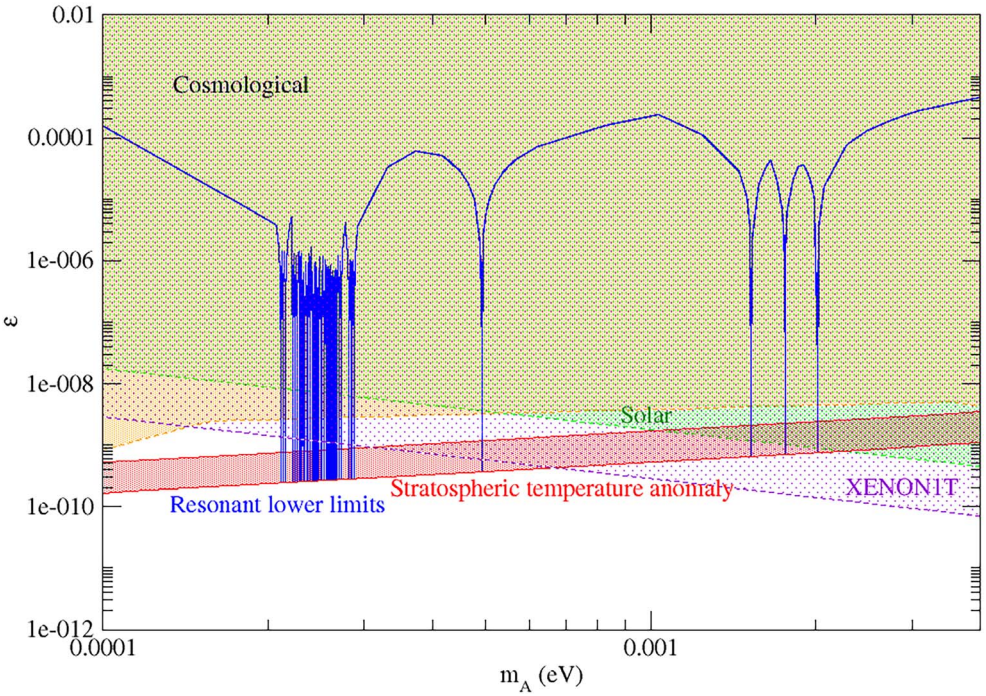

Figure 3. The blue solid line indicates the lower limit of ε, assuming the resonant absorption (rotational excitation) with $\dot{Q} = 0.1$ W m^{-2} originated from oxygen molecules. The red shaded band represents the continuous resonant constraint of ε shown in Figure 2. The orange, green, and violet shaded regions represent the ruled out parameter space based on the cosmological observations in S. J. Witte et al. (2020), solar global analysis in N. Vinyoles et al. (2015), and solar dark photon constraints in the XENON1T experiment (E. Aprile et al. 2022).

be seen in Earth's atmosphere and Pluto's atmosphere (G. R. Gladstone et al. 2016). Therefore, investigating the heating of planets and planetary atmospheres is a possible way to test the DPDM proposal.

3.2. Supermassive Dark Star

It has been suggested that some dark stars heated by dark matter might exist in the early epoch. The original proposal of the supermassive dark star suggests that a massive gas halo can be ignited by WIMP dark matter annihilation (D. Spolyar et al. 2009; K. Freese et al. 2010). The energy input can give a sufficient temperature $T > 10^4$ K and luminosity $L \geqslant 10^9 L_\odot$ for us to observe even in redshift >10 (K. Freese et al. 2010). Recently, a study claims that three possible supermassive dark stars (JADES-GS-z13-0, JADES-GS-z12-0, and JADES-GS-z11-0) might have been observed (C. Ilie et al. 2023). This reveals a possibility of dark matter heating of a massive gas halo in the early Universe. In the DPDM context, the heating of DPDM can also provide sufficient energy to give the required luminosity. The adiabatic contraction would give a high ambient dark matter density according to the relation: $\rho_{DM} \sim 5(n_H/\mathrm{cm}^3)^{0.81}$ GeV cm^{-3} (D. Spolyar et al. 2009). For the average baryonic density $n_H \sim 10^{13}$ cm^{-3}, we have $\rho_{DM} \sim 10^{11}$ GeV cm^{-3}. The size of a supermassive dark star can be as large as 10 au (C. Ilie et al. 2023). Therefore, the total dark matter mass inside the supermassive dark star is $M_{DM} \sim 10^{-3} M_\odot$. Taking the average velocity of the gas particle as $v = \sqrt{3kT/m_H}$ with $T = 10^4$ K and assuming all gas particles have the resonant absorption frequency $\nu_0 \approx \nu$, the heating rate of DPDM is

$$\dot{Q} = M_{DM} n_H \sigma_A v c^2 > 10^9 L_\odot. \quad (13)$$

This shows that the heating of DPDM can also provide the required luminosity for the supermassive dark star observed recently. As the dark matter mass depletion rate is $\dot{M}_{DM} = \dot{Q}/c^2 > 6.7 \times 10^{-5} M_\odot$ yr^{-1}, the accretion rate of dark matter mass larger than the depletion rate is required to maintain the luminosity for a long time.

3.3. Direct Detection of Dark Matter at High Altitude

Since we have shown that only a small amount of DPDM particles would be absorbed in the stratosphere and mesosphere, this provides a window for us to detect dark matter at high altitude. For example, in the stratosphere ($h > 20$ km), less than 40% of DPDM would be absorbed by the stratosphere based on our assumed energy deposition rate. Therefore, detecting the signals of dark matter in the stratosphere would be much more effective. One can design a cavity experiment performed in the stratosphere using a balloon. This can equivalently push the limit of the mixing parameter ε by more than 100 times compared with the experiments performed at sea level if $\tau(0) = 10$. Based on the current constraints of the haloscope experiments (A. Caputo et al. 2021), pushing the limits by 100 times can definitely make the DPDM signal detectable because the revised projected limits would overlap with our constrained $\varepsilon - m_A$ parameter space.

4. Discussion and Conclusion

In this article, I have argued that the atmospheric resonant absorption of DPDM is possible. If the so-called stratospheric temperature anomalies are real phenomena, then our proposal could account for the required energy deposition. The resonant absorption can originate from the rotational and vibrational eigenstate transition of diatomic and triatomic molecules in the atmosphere (A. Arvanitaki et al. 2018). There are many possible resonant absorption energies <0.01 eV in atmospheric

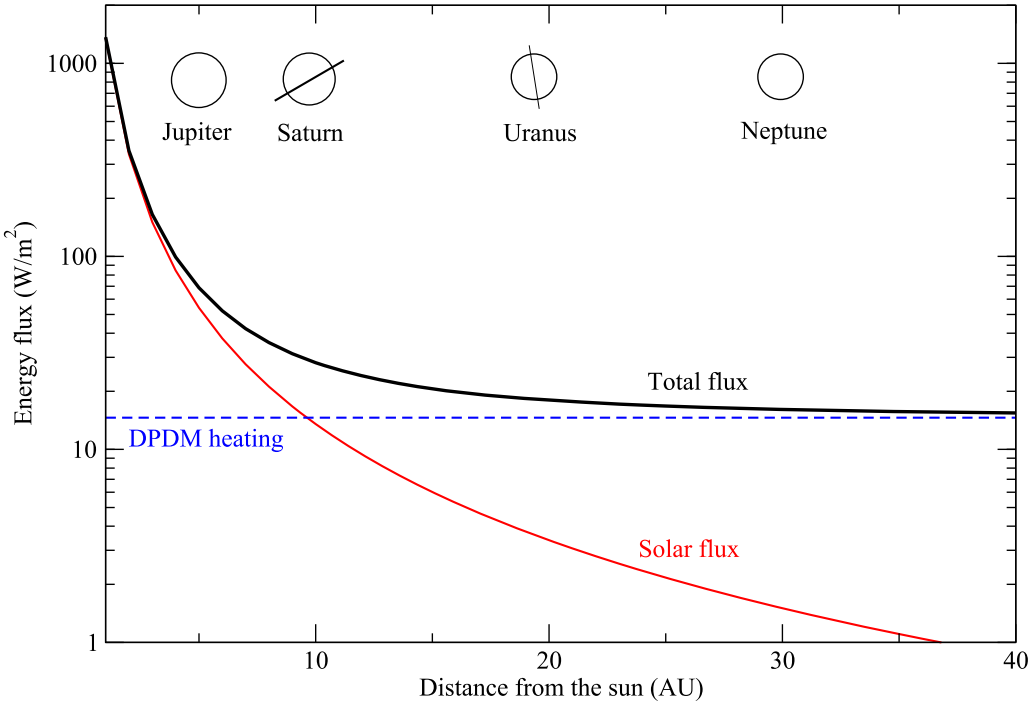

Figure 4. The red solid line and blue dashed line, respectively, represent the solar flux and the heating flux of DPDM. The black solid line represents the total flux by adding the solar flux with the DPDM heating flux. Here, we have neglected the effect of bond albedo for the planets. The positions of the Jovian planets are shown in the figure.

molecules, such as oxygen (J. H. Van Vleck 1947; M. Toureille et al. 2020). In fact, many recent studies have turned to consider DPDM as a highly probable candidate of dark matter so the DPDM model has been put on different experimental tests (J. Chiles et al. 2022; H. An et al. 2023, 2024; F. Bajjali et al. 2023; N. T. Hunt-Smith et al. 2023; S. Knirck et al. 2024; S. Roy & C. E. M. Wagner 2024). Some recent experimental results even favor the existence of a dark photon (N. T. Hunt-Smith et al. 2023). Based on our assumptions, we can get a narrow constrained DPDM mass range $m_A \sim 0.0001$–0.001 eV and the viable range of the mixing parameter ε without violating current astrophysical and cosmological bounds. Note that the cross section σ_A in Equation (4) involves a few approximations, including the value of the partition function assumed. Nevertheless, the order of magnitudes of the allowed ε provide a viable window for strong interaction between dark matter and ordinary matter. It also justifies the possibility of having atmospheric absorption of DPDM.

Previously, we often believed that the interaction between dark matter particles and ordinary matter is extremely small. This is because we have not detected any interaction signal between dark matter and ordinary matter in the ground-based direct-detection experiments. However, this might be a selection effect in which most of the dark matter particles have already been absorbed by the atmosphere. Here, we have discussed the possibility that most of the dark matter particles are absorbed by the atmosphere based on the DPDM model, without adding any new assumptions to the existing DPDM model. Even if the stratospheric temperature anomalies are false or the anomalies do not originate from DPDM heating, our analysis still shows that effective absorption of DPDM in our atmosphere is possible. It would overturn our usual assumption of extremely weak interaction between dark matter and ordinary matter and revive our hope of detecting dark matter directly. Moreover, we have discussed some interesting implications for the effective absorption of DPDM, such as heating of Jovian planets, igniting a supermassive dark star, and performing the cavity experiment at high altitude. These initiate new research directions that can help verify the DPDM model and solve the long-lasting dark matter problem.

Acknowledgments

I thank the anonymous referee for the useful comments. The work described in this paper was partially supported by the Dean's Research Fund of The Education University of Hong Kong (0400W) and the grants from the Research Grants Council of the Hong Kong Special Administrative Region, China (Project Nos. EdUHK 18300922 and EdUHK 18300324).

ORCID iDs

Man Ho Chan https://orcid.org/0000-0001-5088-9117

References

Aalbers, J., Akerib, D. S., Akerlof, C. W., et al. 2023, PhRvL, 131, 041002
Acevedo, J. F., Leane, R. K., & Reilly, A. J. 2024, arXiv:2405.02393
Ackermann, M., Albert, A., Anderson, B., et al. 2015, PhRvL, 115, 231301
Adair, C. M., Altenmüller, K., Anastassopoulos, V., et al. 2022, NatCo, 13, 6180
Adhikari, P., Ajaj, R., Alpizar-Venegas, M., et al. 2022, PhRvL, 128, 011801
ADMX Collaboration 2020, PhRvL, 124, 101303
ADMX Collaboration 2023, PhRvL, 131, 101002
Aguilar, M., Ali Cavasonza, A., Ambrosi, G., et al. 2019, PhRvL, 122, 041102
Ahyoune, S., Álvarez Melcón, A., Arguedas Cuendis, S., et al. 2024, arXiv:2403.07790
Akerib, D. S., Alsum, S., Araújo, H. M., et al. 2017, PhRvL, 118, 021303
Albert, A., Anderson, B., Bechtol, K., et al. 2017, ApJ, 834, 110
Amole, C., Ardid, M., Arnquist, I. J., et al. 2019, PhRvD, 100, 022001
An, H., Ge, S., Guo, W.-Q., et al. 2023, PhRvL, 130, 181001
An, H., Ge, S., Liu, J., & Lu, Z. 2024, arXiv:2402.17140
Aprile, E., Aalbers, J., Agostini, F., et al. 2018, PhRvL, 121, 111302

Aprile, E., Aalbers, J., Agostini, F., et al. 2020, PhRvD, 102, 072004
Aprile, E., Abe, K., Agostini, F., et al. 2022, PhRvD, 106, 022001
Aprile, E., Abe, K., Ahmed Maouloud, S., et al. 2023, PhRvL, 130, 261002
Arcadi, G., Cabo-Almeida, D., Dutra, M., et al. 2024, arXiv:2403.15860
Arias, P., Cadamuro, D., Goodsell, M., et al. 2012, JCAP, 06, 013
Arvanitaki, A., Dimopoulos, S., & Van Tilburg, K. 2018, PhRvX, 8, 041001
Bajjali, F., Dornbusch, S., Ekmedžić, M., et al. 2023, JCAP, 08, 077
Barton, E. J., Hill, C., Yurchenko, S. N., et al. 2017, JQSRT, 187, 453
Beck, G., & Sarkis, M. 2023, PhRvD, 107, 023006
Bertolucci, S., Zioutas, K., Hofmann, S., & Maroudas, M. 2017, PDU, 17, 13
Caputo, A., Millar, A. J., O'Hare, C. A. J., & Vitagliano, E. 2021, PhRvD, 104, 095029
Chan, M. H., & Lee, C. M. 2020, PhRvD, 102, 063017
Chiles, J., Charaev, I., Lasenby, R., et al. 2022, PhRvL, 128, 231802
Fabbrichesi, M., Gabrielli, E., & Lanfranchi, G. 2020, arXiv:2005.01515
Freese, K., Ilie, C., Spolyar, D., Valluri, M., & Bodenheimer, P. 2010, ApJ, 716, 1397
Gladstone, G. R., Stern, S. A., Ennico, K., et al. 2016, Sci, 351, aad8866
Graham, P. W., Mardon, J., & Rajendran, S. 2016, PhRvD, 93, 103520
Harris, G. J., Viti, S., Mussa, H. Y., & Tennyson, J. 1998, JChPh, 109, 7197
Hunt-Smith, N. T., Melnitchouk, W., Sato, N., et al. 2023, JHEP, 09, 096
Ilie, C., Paulin, J., & Freese, K. 2023, PNAS, 120, e2305762120
Ingersoll, A. P. 2020, SSRv, 216, 122
Knirck, S., Hoshino, G., Awida, M. H., et al. 2024, PhRvL, 132, 131004
Kwon, O., Lee, D., Chung, W., et al. 2021, PhRvL, 126, 191802
Labini, F. S., Chrobakova, Z., Capuzzo-Dolcetta, R., & Lopez-Corredoira, M. 2023, ApJ, 945, 3
Li, S.-P., & Xu, X.-J. 2023, JCAP, 09, 009
Li, L., Jiang, X., West, R. A., et al. 2018, NatCo, 9, 3709
Markham, S., & Stevenson, D. 2021, PSJ, 2, 146
Nelson, A. E., & Scholtz, J. 2011, PhRvD, 84, 103501
Neuenschwander, B. A., Müller, S., & Helled, R. 2024, A&A, 684, A191
Neufeld, D. A., Farrar, G. R., & McKee, C. F. 2018, ApJ, 866, 111
Redondo, J., & Postma, M. 2009, JCAP, 02, 005
Roy, S., & Wagner, C. E. M. 2024, JHEP, 04, 106
Spolyar, D., Bodenheimer, P., Freese, K., & Gondolo, P. 2009, ApJ, 705, 1031
Toureille, M., Béguier, S., Odintsova, T. A., et al. 2020, JQSRT, 242, 106709
Van Vleck, J. H. 1947, PhRv, 71, 413
Vinyoles, N., Serenelli, A., Villante, F. L., et al. 2015, JCAP, 10, 015
Welbanks, L., Bell, T. J., Beatty, T. G., et al. 2024, Natur, 630, 836
Witte, S. J., Rosauro-Alcaraz, S., McDermott, S. D., & Poulin, V. 2020, JHEP, 06, 132
Witze, A. 2015, Natur, 523, 389
Yang, B., Yoon, H., Ahn, M., Lee, Y., & Yoo, J. 2023, PhRvL, 131, 081801
Zak, E. J. 2022, arXiv:2203.09241
Zhitnitsky, A., & Maroudas, M. 2025, Symm, 17, 79
Zioutas, K., Argiriou, A., Fischer, H., et al. 2020, PDU, 28, 100497